Iranian Journal of Numerical Analysis and Optimization
Vol. 16, No. 4, 2026, pp 1221–1238
https://doi.org/10.22067/ijnao.2026.97767.1839
https://ijnao.um.ac.ir/

Research Article

Second-kind Chebyshev spectral Petrov–Galerkin scheme for solving the time-fractional Euler–Bernoulli beam equation

Y.H. Youssri*, and M.M. Muttardi

Abstract

This work introduces a novel Petrov–Galerkin spectral technique designed to investigate vibrational behavior in fourth-order time-fractional Euler–Bernoulli beams with pinned-pinned boundary conditions. A tailored basis comprising shifted second-kind Chebyshev polynomials is developed, which automatically fulfills homogeneous boundary constraints, thus lowering computational demands. By selecting test functions from the same Chebyshev family, the Petrov–Galerkin framework converts the fractional partial differential equation into a structured algebraic system that can be efficiently resolved through Gaussian elimination. The proposed scheme delivers exponential convergence for sufficiently smooth solutions, exhibits low numerical dispersion, and remains straightforward to implement even for high-order problems. Rigorous error estimates in both L_∞ and L_2 norms ensure theoretical reliability. Computational tests, including a case lacking a closed-form exact solution, validate the precision and computational efficiency of the approach.

*Corresponding author

Received 9 February 2026; revised 14 May 2026; accepted 24 May 2026

Youssri Hassan Youssri
Department of Mathematics, Faculty of Science, Cairo University, Giza 12613, Egypt. e-mail: youssri@cu.edu.eg

Maha Muftah Muttardi
Mathematics and Actuarial Science Department, School of Science and Engineering, The American University in Cairo, New Cairo 11835, Egypt. e-mail: mahamuttardi@aucegypt.edu

How to cite this article
Youssri, Y.H. and Muttardi, M.M., Second-kind Chebyshev spectral Petrov–Galerkin scheme for solving the time-fractional Euler–Bernoulli beam equation. *Iran. J. Numer. Anal. Optim.*, 2026; 16(4): 1221-1238. https://doi.org/10.22067/ijnao.2026.97767.1839

AMS subject classifications (2020): Primary 65M70, 42C05; Secondary 65G99, 35R11.

Keywords: Time-fractional fourth-order partial differential equations; Chebyshev polynomials; Petrov–Galerkin method; Error analysis.

1 Introduction

Research interest in fractional differential equations has grown considerably, owing to their capacity to represent intricate physical processes exhibiting memory effects and hereditary characteristics across diverse domains such as wave dynamics, turbulent flows, signal analysis, and flow through porous structures [17, 23]. For treatments of both fractional and classical differential problems, refer to [14, 25]. Incorporating fractional derivatives of orders in $(0, 1)$ into the temporal component of the classical diffusion equation yields fractional-order differential models. Substantial theoretical and computational efforts have been devoted to the time-fractional fourth-order sub-diffusion equation. Notably, closed-form analytical solutions for most fractional differential equations remain unavailable [28]. Recent progress in numerical techniques for fractional differential equations is documented in [6, 31, 32, 33, 34]. Recent investigations have highlighted the effectiveness of hybrid spectral techniques combined with cardinal functions in delivering highly accurate numerical approximations for challenging fractional models, including multi-dimensional Rayleigh–Stokes systems [18], time-fractional three-dimensional Sobolev equations [19], and variable-order two-dimensional Wu–Zhang systems [16]. Beam models serve to characterize transversely oscillating beams subjected to external forcing, as discussed in [15]. Among these, the Euler–Bernoulli beam formulation represents one of the most fundamental frameworks capable of addressing a wide range of engineering challenges [10]. This model explicitly accounts for undamped transverse oscillations of a straight, flexible beam without support contributions.

A variety of numerical strategies have been proposed to tackle the Euler–Bernoulli equation, such as finite difference schemes [12], alternating group explicit iterative procedures [7], alternating direction implicit methods [13], the Legendre–Laguerre–Galerkin technique [11], Adomian decomposition approaches [30], and Petrov–Galerkin formulations [36].

Spectral methods are widely regarded as among the most accurate numerical or semi-analytical tools for partial differential equations (PDEs), provided they are properly implemented, due to their high-order convergence properties. Standard spectral and weighted residual techniques have been extensively investigated for solving stochastic PDEs, fractional Lane–Emden equations, linear hyperbolic first-order PDEs, one- and two-dimensional heat equations, second-order diffusion problems, and other recent spectral approaches for diverse PDE classes [1, 2, 3, 5, 8, 20, 26, 35, 38].

Selecting suitable basis functions is critical for the success of spectral approximations. Among the many options, Chebyshev polynomials of the first kind have proven particularly effective due to their advantageous properties and trigonometric representation. Readers interested in Chebyshev polynomials may consult [21] for foundational material. In recent years, Chebyshev polynomials have been successfully employed within spectral frameworks to address numerous differential problems; see, for instance, [9, 22].

The central objective of this study is to develop an explicit Chebyshev Petrov–Galerkin method for solving a time-fractional fourth-order uniform Euler–Bernoulli beam problem with pinned-pinned boundary conditions. The remainder of this manuscript is organized as follows: Section 2 reviews essential concepts from fractional calculus and key properties of shifted second-kind Chebyshev polynomials (S2KCPs). Section 3 presents the core spectral methodology for addressing the underlying fractional PDE. Section 4 addresses the estimation of truncation errors. Section 5 provides numerical illustrations with comparative assessments. Finally, Section 6 offers concluding observations.

2 Fundamental relations

This section introduces the Caputo fractional derivative and relevant characteristics of S2KCPs.

2.1 Caputo fractional derivative

Definition 1. [23] The Caputo fractional derivative of order $r > 0$ is given by

$$D_t^r \chi(t) = \frac{1}{\Gamma(s-r)} \int_0^t (t-z)^{s-r-1} \chi^{(s)}(z)\, dz, \quad t > 0, \tag{1}$$

where $s = \lceil r \rceil$ (the smallest integer greater than or equal to r), ensuring $s-1 < r \leq s$. This convention aligns with the standard Caputo notation $n-1 < \alpha \leq n$ commonly adopted in the literature, thereby avoiding ambiguity with the alternative form $s-1 \leq r < s$.

The operator D_t^r possesses the following properties:

$$D_t^r b = 0 \quad (b \text{ is a constant}), \tag{2}$$

$$D_t^r\, t^s = \begin{cases} 0, & \text{if } s \in \mathbb{N}_0 \text{ and } s < \lceil r \rceil, \\ \frac{\Gamma(s+1)}{\Gamma(s-r+1)}\, t^{s-r}, & \text{if } s \in \mathbb{N}_0 \text{ and } s \geq \lceil r \rceil, \end{cases} \tag{3}$$

where $\mathbb{N} = \{1, 2, 3, \ldots\}$ and $\mathbb{N}_0 = \{0\} \cup \mathbb{N}$.

2.2 Essential properties of S2KCPs

The S2KCPs defined on $[0, 1]$ are given by $\{U_m^*(\iota) = U_m(2\iota - 1) : m \in \mathbb{N}_0\}$, with the explicit representation [9]:

$$U_m^*(\iota) = m \sum_{k=0}^{m} \frac{(-1)^{m+k}\, 2^{2k}\, (m+k+1)!}{(m-k)!\, (2k+1)!}\, \iota^k, \quad m \geq 0. \tag{4}$$

These polynomials satisfy an orthogonality relation with respect to the weight $\hat{w}(\iota) = \sqrt{\iota(1-\iota)}$:

$$\int_0^1 \hat{w}(\iota)\, U_m^*(\iota)\, U_n^*(\iota)\, d\iota = g_{m,n}, \tag{5}$$

where

$$g_{m,n} = \begin{cases} \frac{\pi}{8}, & m = n, \\ 0, & m \neq n. \end{cases} \tag{6}$$

Remark 1. The weight function $\hat{w}(\iota) = \sqrt{\iota(1-\iota)}$ arises from the standard Chebyshev weight $\sqrt{1-x^2}$ on $[-1, 1]$ via the affine transformation $x = 2\iota - 1$, since $dx = 2\, d\iota$ and $\sqrt{1-x^2} = 2\sqrt{\iota(1-\iota)}$. The factor of 2 is incorporated into the normalization constant $g_{m,n}$.

The three-term recurrence relation reads as follows:

$$U_n^*(\iota) = 2(2\iota - 1)U_{n-1}^*(\iota) - U_{n-2}^*(\iota), \quad U_0^* = 1,\ U_1^* = 2\iota - 1. \tag{7}$$

The inversion formula [9] is expressed as

$$\iota^j = \frac{4\Gamma(j+\frac{3}{2})}{\sqrt{\pi}} \sum_{p=0}^{j} \frac{j!(1+p)!}{p!(j-p)!(2+j+p)!}\, U_p^*(\iota), \quad j \geq 0. \tag{8}$$

3 Petrov–Galerkin approach for fourth-order time-fractional PDEs

We examine the time-fractional fourth-order PDE (TF4PDE) [24]:

$$D_t^{\alpha}\nu(\iota,t)+\beta\,\frac{\partial^4\nu(\iota,t)}{\partial\iota^4}=f(\iota,t),\quad 0<\alpha\le 1,\ 0<\iota,t\le 1, \tag{9}$$

subject to the initial and boundary conditions:

$$\nu(\iota,0)=p_1(\iota),\quad \nu_t(\iota,0)=p_2(\iota),\quad 0<\iota\le 1, \tag{10}$$

$$\nu(0,t)=\nu(1,t)=\nu_\iota(0,t)=\nu_\iota(1,t)=0,\quad 0<t\le 1. \tag{11}$$

Here, f denotes a prescribed source term and $\beta>0$ is a constant parameter.

3.1 Trial functions

We construct basis functions that inherently satisfy the homogeneous boundary constraints:

$$\varphi_i(\iota)=a_1U_i^*+a_2U_{i+1}^*+a_3U_{i+2}^*+a_4U_{i+3}^*+U_{i+4}^*, \tag{12}$$

$$\psi_j(t)=U_j^*(t). \tag{13}$$

Utilizing the identities $U_k^*(0)=(-1)^k(k+1)$, $U_k^{*'}(0)=\frac{2}{3}(-1)^{k-1}(k)_3$, $U_k^*(1)=k+1$, and $U_k^{*'}(1)=\frac{2}{3}(k)_3$, we enforce $\varphi_i(0)=\varphi_i(1)=\varphi_i'(0)=\varphi_i'(1)=0$, which yields a linear system for the coefficients $a_1,\dots,a_4$:

$$\begin{aligned}a_1(-1)^i(i+1)+a_2(-1)^{i+1}(i+2)+a_3(-1)^{i+2}(i+3)&\\ +a_4(-1)^{i+3}(i+4)+(-1)^{i+4}(i+5)&=0,\end{aligned} \tag{14}$$

$$a_1(i+1)+a_2(i+2)+a_3(i+3)+a_4(i+4)+(i+5)=0, \tag{15}$$

$$\begin{aligned}a_1(i)_3(-1)^{i-1}+a_2(i+1)_3(-1)^{i}+a_3(i+2)_3(-1)^{i+1}&\\ +a_4(i+3)_3(-1)^{i+2}+(i+4)_3(-1)^{i+3}&=0,\end{aligned} \tag{16}$$

$$a_1(i)_3+a_2(i+1)_3+a_3(i+2)_3+a_4(i+3)_3+(i+4)_3=0. \tag{17}$$

Solving this 4×4 linear system (for instance, via Gaussian elimination) produces the compact representation:

$$\varphi_i(\iota) = \frac{(i+4)(i+5)}{(i+1)(i+2)} U_i^* - 2\frac{i+5}{i+2} U_{i+2}^* + U_{i+4}^*. \tag{18}$$

The approximate solution takes the form:

$$\nu^M(\iota, t) = \sum_{i=0}^{M} \sum_{j=0}^{M} c_{ij}\, \varphi_i(\iota)\psi_j(t). \tag{19}$$

Substituting this expansion into (9) and applying the Petrov–Galerkin procedure with test functions $\psi_{r,s}(\iota, t) = U_r^*(\iota)U_s^*(t)$ leads to

$$\left(D_t^\alpha \nu^M + \beta \partial_\iota^4 \nu^M - f,\ U_r^* U_s^*\right)_\omega = 0, \tag{20}$$

where $\omega(\iota, t) = \hat{w}(\iota)\hat{w}(t)$. Introducing the matrices,

$$\begin{aligned}
\hat{\boldsymbol{A}} &= (a_{ir}), \quad a_{ir} = (\varphi_i, U_r^*)_{\hat{w}}, \\
\hat{\boldsymbol{B}} &= (b_{sj}), \quad b_{sj} = (U_s^*, D_t^\alpha U_j^*)_{\hat{w}}, \\
\hat{\boldsymbol{H}} &= (\bar{h}_{ir}), \quad \bar{h}_{ir} = (\partial_\iota^4 \varphi_i, U_r^*)_{\hat{w}}, \\
\hat{\boldsymbol{K}} &= (k_{sj}), \quad k_{sj} = (U_s^*, U_j^*)_{\hat{w}}, \\
\hat{\boldsymbol{F}} &= (f_{rs}), \quad f_{rs} = (f, U_r^* U_s^*)_\omega,
\end{aligned}$$

with dimensions $\hat{\boldsymbol{A}}, \hat{\boldsymbol{H}} \in \mathbb{R}^{(M+1)\times(M+1)}$, $\hat{\boldsymbol{B}}, \hat{\boldsymbol{K}} \in \mathbb{R}^{M\times(M+1)}$, $\hat{\boldsymbol{F}} \in \mathbb{R}^{(M+1)\times M}$, and $\hat{\boldsymbol{C}} = (c_{ij}) \in \mathbb{R}^{(M+1)\times(M+1)}$, the resulting system can be written as follows:

$$\hat{\boldsymbol{A}}\hat{\boldsymbol{C}}\hat{\boldsymbol{B}}^\top + \beta\, \hat{\boldsymbol{H}}\hat{\boldsymbol{C}}\hat{\boldsymbol{K}}^\top = \hat{\boldsymbol{F}}. \tag{21}$$

The matrix products are dimensionally compatible: both $\hat{\boldsymbol{A}}\hat{\boldsymbol{C}}\hat{\boldsymbol{B}}^\top$ and $\hat{\boldsymbol{H}}\hat{\boldsymbol{C}}\hat{\boldsymbol{K}}^\top$ yield matrices of size $(M+1) \times M$.

Corollary 1. [4] The qth derivative of U_j^* admits the representation:

$$D^q U_j^*(\iota) = \sum_{\substack{p=0 \\ (q+p+j)\ \text{even}}}^{j-q} \lambda_{j,p,q}\, U_p^*(\iota), \tag{22}$$

where $\lambda_{j,p,q} = \dfrac{j\, 2^{2q}\, (q)_{\frac{1}{2}(j-p-q)}}{\left(\frac{1}{2}(j-p-q)\right)!\, \left(\frac{1}{2}(q+p+j)\right)_{1-q}}$.

3.2 Petrov–Galerkin solution

Theorem 1. The entries of the matrices appearing in (21) are given by

$$\begin{aligned}
k_{sj} &= g_{s,j},\\
a_{ir} &= g_{i+4,r} - \frac{2(i+2)(2i^2+8i+15)}{(i+1)(2i^2+4i+3)} g_{i+2,r} + \frac{(i+3)(2i^2+12i+19)}{(i+1)(2i^2+4i+3)} g_{i,r},\\
\bar{h}_{ir} &= \begin{cases} 128\pi(i+1)(i+2)(i+3)(i+4), & i=r,\\ \frac{256\pi i(i+2)(2i^4+18i^3+43i^2+63i+54)}{2i^2+4i+3}, & i-r=2,\\ \frac{384\pi(i-1)i(2i^5+24i^4+81i^3+218i^2+489i+474)}{(i+1)(2i^2+4i+3)}, & i-r=4,\\ 0, & \text{otherwise}, \end{cases}\\
b_{sj} &= (-1)^{j+1} j^2 \pi\, \Gamma\left(\tfrac{3}{2}-\alpha\right)\ {}_4F_3\left(\left.\begin{matrix} 1, 1-j, j+1, \frac{3}{2}-\alpha \\ \frac{3}{2}, -s-\alpha+2, s-\alpha+2 \end{matrix}\right| 1\right).
\end{aligned} \tag{23}$$

Proof. The formulas for k_{sj} and a_{ir} follow directly from the orthogonality relation (5) together with the compact basis expression (18). To obtain $\bar{h}_{ir}$, apply Corollary 1 with $q=4$ to $\partial_t^4 \varphi_i$ and exploit orthogonality. For b_{sj}, combine (3) and (4) to write

$$\begin{aligned}
b_{sj} &= \int_0^1 \left[D_t^\alpha U_j^*(t)\right] U_s^*(t) \hat{w}(t)\, dt\\
&= js \sum_{k=0}^{j} \sum_{n=0}^{s} \frac{(-1)^{j-k} 2^{2k} (j+k-1)!\, \Gamma(k+1)\, (-1)^{s-n} 2^{2n} (s+n-1)!}{(j-k)!(2k)!\, \Gamma(k-\alpha+1)(s-n)!(2n)!}\\
&\quad \int_0^1 \frac{t^{k+n-\alpha}}{\sqrt{t(1-t)}}\, dt.
\end{aligned} \tag{24}$$

Evaluating the resulting beta integral and simplifying the expression leads to the unified ${}_4F_3$ hypergeometric representation. □

Remark 2. The Petrov–Galerkin framework provides three principal benefits: (i) the compact basis (18) enforces boundary conditions exactly, thereby eliminating the need for penalty terms; (ii) the operational matrices exhibit sparse, banded structure, enabling assembly with $O(M^2)$ complexity; (iii) exponential convergence is attained for sufficiently smooth solutions, offering superior accuracy compared to finite-difference or finite-element approaches when high precision is required.

4 Error analysis

We examine the approximation error $\nu - \nu^M$ measured in both L_∞ and L_2 norms.

4.1 L_∞-norm error analysis

Let $\hat{\nu}^M$ denote the interpolant of ν at the Chebyshev nodes. Then

$$\|\nu - \nu^M\|_\infty \leq \|\nu - \hat{\nu}^M\|_\infty. \tag{25}$$

Applying the two-dimensional Taylor remainder formula yields

$$\begin{aligned}\nu - \hat{\nu}^M = {} & \frac{\partial^{M+1}\nu(\eta, t)}{\partial\iota^{M+1}(M+1)!}\prod_{i=0}^{M}(\iota - \iota_i) + \frac{\partial^{M+1}\nu(\iota, \mu)}{\partial t^{M+1}(M+1)!}\prod_{j=0}^{M}(t - t_j) \\ & + \frac{\partial^{2M+2}\nu(\hat{\eta}, \hat{\mu})}{\partial\iota^{M+1}\partial t^{M+1}((M+1)!)^2}\prod_{i=0}^{M}(\iota - \iota_i)\prod_{j=0}^{M}(t - t_j),\end{aligned} \tag{26}$$

where the third term carries a *positive* sign, consistent with the standard remainder expression. Bounding the derivatives by constants g_1, g_2, g_3 and minimizing the nodal polynomials through Chebyshev node selection leads to

$$\|\nu - \nu^M\|_\infty \leq g_1\frac{(1/2)^{M+1}\Upsilon_M}{\bar{\zeta}_M(M+1)!} + g_2\frac{(1/2)^{M+1}}{\hat{U}_M(M+1)!} + g_3\frac{(1/4)^{M+1}\Upsilon_M}{\bar{\zeta}_M\hat{U}_M((M+1)!)^2}. \tag{27}$$

4.2 L_2-norm error analysis

Theorem 2. Assume that $\nu^M \in \Lambda^M$ represents the approximate solution and that $\partial^{i+j}\nu/\partial\iota^i\partial t^j \in C(\Omega)$ for $i, j \leq M+1$. Define

$$\mathcal{L}_M = \sup_{(\iota,t)\in\Omega}\left|\frac{\partial^{2(M+1)}\nu}{\partial\iota^{M+1}\partial t^{M+1}}\right|. \tag{28}$$

Then

$$\|\nu - \nu^M\|_2 \leq \mathfrak{n}\,\frac{\mathcal{L}_M}{M^{3/4}(\Gamma(M+2))^2}, \tag{29}$$

where $\mathfrak{n} > 0$ denotes a generic constant independent of M (explicitly, $\mathfrak{n} = \sqrt{\pi}\,\sup_{z\geq 1}\mathbf{o}_z^{a,b}$ as given in [39]).

Proof. Exploiting the best approximation property together with a Taylor expansion gives

$$\|\nu - \nu^M\|_2^2 \leq \int_0^1\int_0^1 \frac{\mathcal{L}_M^2\,\iota^{2(M+1)}t^{2(M+1)}}{(\Gamma(M+2))^4}\hat{w}(\iota)\hat{w}(t)\,d\iota\,dt. \tag{30}$$

Evaluating the beta integrals and applying the gamma ratio bound from [39] yield the stated result with the explicit constant $\mathfrak{n}$. □

Theorem 3. Under the assumptions of Theorem 2, define

$$\mathcal{U}_{M,m} = \sup_{\Omega}\left|\frac{\partial^{2M-m+2}\nu}{\partial\iota^{M-m+1}\partial t^{M+1}}\right|, \quad m = 1,\dots,4. \tag{31}$$

Then

$$\left\|\frac{\partial^m(\nu-\nu^M)}{\partial\iota^m}\right\|_2 \leq \mathfrak{n}\,\frac{\mathcal{U}_{M,m}}{(2(M-m)+3)^{1/2}M^{1/4}\Gamma(M+2)\Gamma(M-m+2)}. \tag{32}$$

Theorem 4. If $D_t^{\alpha}\nu \in C(\Omega)$ and

$$\mathcal{P}_{M,\alpha} = \sup_{\Omega}\left|\frac{\partial^{2M-\alpha+2}\nu}{\partial\iota^{M+1}\partial t^{M-\alpha+1}}\right|, \tag{33}$$

then

$$\|D_t^{\alpha}(\nu-\nu^M)\|_2 \leq \mathfrak{n}\,\frac{\mathcal{P}_{M,\alpha}}{(2M+3)^{1/2}(M-\alpha)^{1/4}\Gamma(M+2)\Gamma(M-\alpha+2)}. \tag{34}$$

Theorem 5. The residual $\mathbf{R} = D_t^{\alpha}\nu^M + \beta\partial_\iota^4\nu^M - f$ satisfies the bound:

$$\begin{aligned}\|\mathbf{R}\|_2 \leq \mathfrak{n}\Bigg[&\frac{\mathcal{P}_{M,\alpha}}{(2M+3)^{1/2}(M-\alpha)^{1/4}\Gamma(M+2)\Gamma(M-\alpha+2)}\\ &+\beta\,\frac{\mathcal{U}_{M,4}}{(2M-5)^{1/2}M^{1/4}\Gamma(M+2)\Gamma(M-2)}\Bigg].\end{aligned} \tag{35}$$

Consequently, $\|\mathbf{R}\|_2 \to 0$ as $M \to \infty$, with the constant β explicitly retained in the fourth-derivative contribution.

5 Illustrative examples

This section demonstrates the practical applicability of the proposed method through three numerical test cases. All computations were carried out using Mathematica 12 on a workstation equipped with an Intel(R) Core(TM) i7-8700 CPU @ 3.20 GHz and 16.0 GB of RAM.

Example 1. [24, 27, 29] Consider the TF4PDE given by

$$D_t^{\alpha}\nu(\iota,t)+\beta\,\frac{\partial^4\nu(\iota,t)}{\partial\iota^4}=f(\iota,t),\quad 0<\alpha\leq 1, \tag{36}$$

subject to the initial and boundary conditions

$$\begin{aligned}&\nu(\iota,0)=\sin(\pi\,\iota),\quad 0<\iota\leq 1,\\ &\nu(0,t)=\nu(1,t)=\nu_{\iota}(0,t)=\nu_{\iota}(1,t)=0,\quad 0<t\leq 1,\end{aligned} \tag{37}$$

where the source term is $f(\iota,t)=\left(\frac{1}{\Gamma(2-\alpha)}\,t^{1-\alpha}+\beta\,\pi^4\,(t+1)\right)\sin(\pi\,\iota)$ and the exact solution is $\nu(\iota,t)=(t+1)\,(1-\iota)\,\sin(\pi\,\iota)$.

Table 1 presents a comparison of the maximum absolute error (MAE) between the proposed scheme and existing methods from several references [24, 27, 29] at $\alpha=0.5$. Table 2 examines how the MAE evolves for the proposed method as M (the number of basis terms) varies, with α fixed at 0.5.

Table 3 explores the variation of MAE across different time instances (t) within the interval $0<t<1$, using the proposed method with $\alpha=0.1$ and $M=12$. This table underscores the capability of the method to deliver highly accurate results even with a relatively small number of basis functions. Figures 1, 2, and 3 display the exact and computed solutions for $M=12$ at various values of α. Figure 4 illustrates the absolute error distribution for Example 1 with $M=12$.

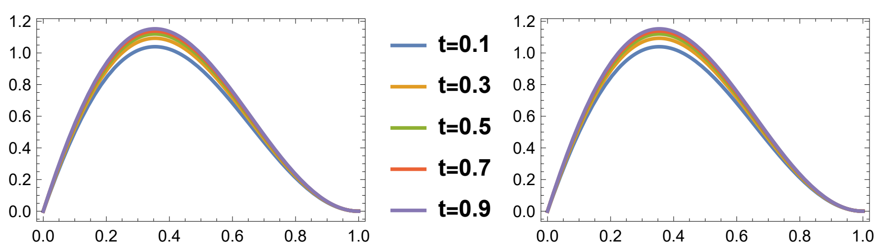

Figure 1: The exact (left) and approximate (right) solutions of Example 1 for $\alpha=0.1$

Table 1: Comparison of the MAE for Example 1.

At $\Lambda t=0.00001$, $m=40$, $n=500$			At $M=12$
Method in [24]	Method in [29]	Method in [27]	Our method
4.69×10^{-8}	1.43×10^{-4}	2.32×10^{-4}	2.22×10^{-11}

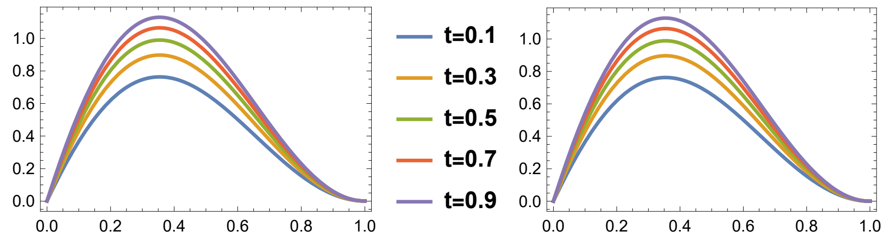

Figure 2: The exact (left) and approximate (right) solutions of Example 1 for $\alpha = 0.5$

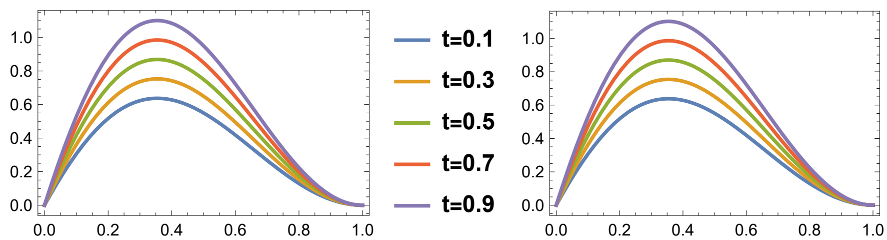

Figure 3: The exact (left) and approximate (right) solutions of Example 1 for $\alpha = 1$

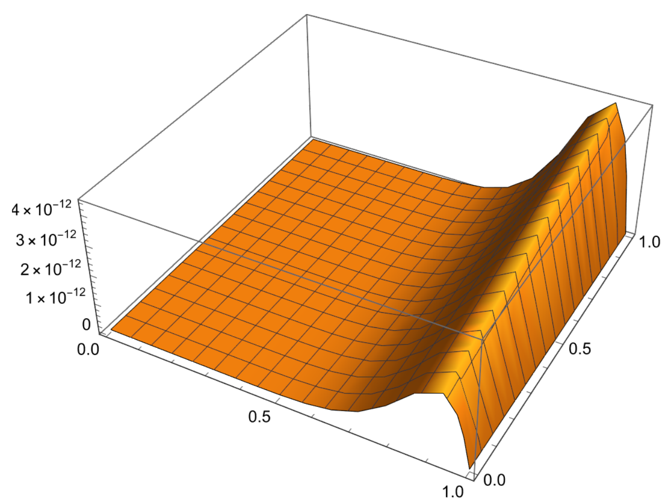

Figure 4: Absolute error example 1 when $M = 12$

Table 2: MAE for Example 1.

M	2	4	6	8	10	12
Error	2.51×10^{-2}	4.62×10^{-4}	7.82×10^{-6}	5.35×10^{-8}	7.06×10^{-10}	2.22×10^{-11}

Example 2. [24] Consider the TF4PDE of the form

Table 3: MAE for Example 1.

(x,t)	$(x,0.1)$	$(x,0.3)$	$(x,0.5)$	$(x,0.7)$	$(x,0.9)$
Error	2.43×10^{-13}	4.52×10^{-12}	4.92×10^{-12}	2.22×10^{-12}	2.22×10^{-12}

$$D_t^{\alpha}\nu(\iota,t)+\beta\,\frac{\partial^4\nu(\iota,t)}{\partial\iota^4}=f(\iota,t),\quad 0<\alpha\le 1, \tag{38}$$

subject to the initial and boundary conditions

$$\begin{aligned}&\nu(\iota,0)=0,\quad 0<\iota\le 1,\\&\nu(0,t)=\nu(1,t)=\nu_{\iota}(0,t)=\nu_{\iota}(1,t)=0,\quad 0<t\le 1,\end{aligned} \tag{39}$$

where $f(\iota,t)=\left(\frac{2}{\Gamma(3-\alpha)}\,t^{2-\alpha}+16\,\beta\,\pi^4\,t^2\right)\sin(2\,\pi\,\iota)$ and the exact solution is $\nu(\iota,t)=t^2\,\sin(2\,\pi\,\iota)$. Table 4 compares the MAE obtained by the proposed method with that from [24] for several values of α. Figures 5, 6, and 7 show the exact and computed solutions for $M=12$ at different α values. Figure 8 displays the absolute error for Example 2 with $M=12$.

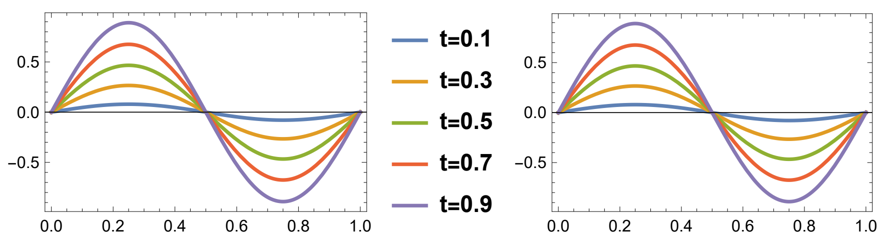

Figure 5: The exact (left) and approximate (right) solutions of Example 2 for $\alpha=0.1$

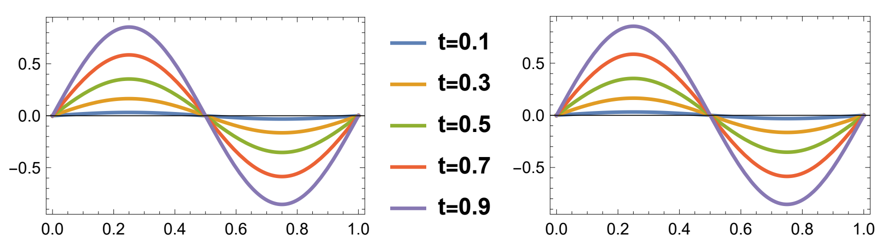

Figure 6: The exact (left) and approximate (right) solutions of Example 2 for $\alpha=0.5$

Example 3. Consider the TF4PDE given by

$$D_t^{\alpha}\nu(\iota,t)+\beta\,\frac{\partial^4\nu(\iota,t)}{\partial\iota^4}=f(\iota,t),\quad 0<\alpha\le 1, \tag{40}$$

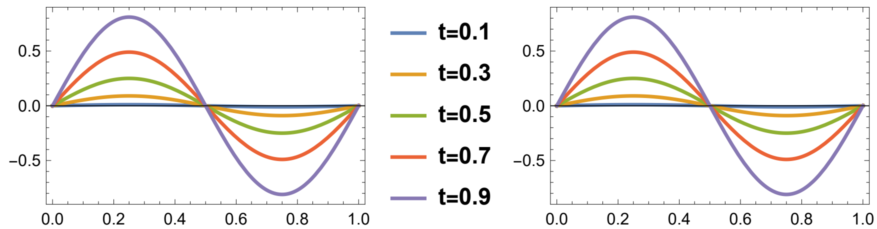

Figure 7: The exact (left) and approximate (right) solutions of Example 2 for $\alpha = 1$

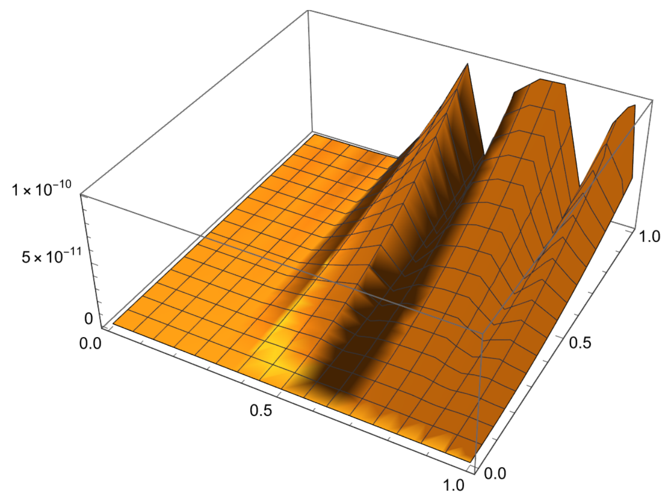

Figure 8: Absolute error example 2 when $M = 12$

Table 4: Comparison of the MAE for Example 2.

α	Method in [24] at $m = 200$, $n = 160$	Our method at $M = 12$
0.4	7.3899×10^{-8}	2.36×10^{-10}
0.5	1.4865×10^{-7}	5.29×10^{-10}
0.7	5.7410×10^{-7}	3.67×10^{-10}

subject to the initial and boundary conditions

$$\begin{aligned} &\nu(\iota, 0) = \sin(\pi\,\iota), \quad 0 < \iota \le 1, \\ &\nu(0,t) = \nu(1,t) = \nu_\iota(0,t) = \nu_\iota(1,t) = 0, \quad 0 < t \le 1, \end{aligned} \tag{41}$$

where the source term $f(\iota, t)$ is selected so that the exact solution is $\nu(\iota, t) = e^{\alpha\, t} \sin(\pi\,\iota)$. Since a closed-form expression for f is not readily available, we evaluate it numerically using the definition of the Caputo derivative. Table 5 reports the MAE for various values of M with $\alpha = 0.9$, demonstrating the method's ability to achieve high accuracy even with modest M.

Table 6 presents the MAE at different time levels t for $\alpha = 0.5$ and $M = 12$ over $0 < \iota < 1$, confirming that the computed solution closely matches the exact one.

Table 5: MAE for Example 3.

M	2	4	6	8	10	12
Error	6.36×10^{-2}	1.00×10^{-3}	5.92×10^{-6}	5.00×10^{-8}	3.70×10^{-10}	2.08×10^{-12}

Table 6: MAE for Example 3.

(x,t)	$(x,0.1)$	$(x,0.3)$	$(x,0.5)$	$(x,0.7)$	$(x,0.9)$
Error	1.32×10^{-12}	1.46×10^{-12}	1.62×10^{-12}	1.79×10^{-12}	1.16×10^{-12}

6 Concluding remarks

This study has addressed the vibrational analysis of a fourth-order time-fractional Euler–Bernoulli beam with pinned-pinned boundary conditions. A novel Petrov–Galerkin spectral framework was developed for this purpose. The approach employs a compact basis formed from Chebyshev polynomials of the second kind to represent the beam displacement. The governing fractional PDE was then transformed into a system of algebraic equations via the Petrov–Galerkin procedure. These equations, involving unknown expansion coefficients characterizing the beam response, were solved efficiently using Gaussian elimination, which is well-suited to the resulting structured system. The method was validated through three numerical examples, including one lacking a known closed-form solution. The computational results confirm that the proposed scheme delivers both high accuracy and computational efficiency.

Potential directions for future work:

- Generalization to variable-order fractional derivatives and nonlinear beam formulations incorporating geometric or material nonlinearities.
- Development of adaptive refinement strategies for solutions exhibiting low regularity or sharp boundary layers.
- Implementation of parallel algorithms and GPU acceleration to handle large-scale three-dimensional beam networks and enable real-time simulations.

- Extension to inverse problems, such as the identification of fractional orders or material parameters from measured vibration data.
- Integration with machine learning methodologies for structural health monitoring and damage detection in fractional viscoelastic structures.

Conflict of interest

The authors declare no conflicts of interest.

Funding

This research received no external funding.

References

[1] Abbasov, Z.D. and Youssri, Y.H. *Fibonacci collocation spectral method and error analysis for heat conduction waves in an n-dimensional domain*, Open J. Math. Sci., 10 (2026), 341–364.

[2] Abd-Elhameed, W.M. and Alkenedri, A.M. *Spectral solutions of linear and nonlinear BVPs using certain Jacobi polynomials generalizing third- and fourth-kinds of Chebyshev polynomials*, CMES-Comp. Model. Eng. Sci., 126(3) (2021), 955–989.

[3] Abd-Elhameed, W.M. and Alkenedri, A.M. *New formulas for the repeated integrals of some Jacobi polynomials: Spectral solutions of even-order boundary value problems*, Int. J. Appl. Comput. Math., 7(4) (2021), 166.

[4] Abd-Elhameed, W.M., Machado, J.A.T. and Youssri, Y.H. *Hypergeometric fractional derivatives formula of shifted Chebyshev polynomials: Tau algorithm for a type of fractional delay differential equations*, Int. J. Nonlinear Sci. Numer. Simul., 23(7-8) (2022), 1253–1268.

[5] Abdelghany, E.M., Abd-Elhameed, W.M., Moatimid, G.M., Youssri, Y.H. and Atta, A.G. *A tau approach for solving time-fractional heat equation based on the shifted sixth-kind Chebyshev polynomials*, Symmetry, 15(3) (2023), 594.

[6] Ahmad, S., Ullah, A., Akgül, A. and De la Sen, M. *A novel homotopy perturbation method with applications to nonlinear fractional-order KdV and Burgers equation with exponential-decay kernel*, J. Function Spaces, 2021(1) (2021), 8770488.

[7] Andrade, C. and McKee, S. *High accuracy a.d.i. methods for fourth-order parabolic equations with variable coefficients*, J. Comput. Appl. Math., 3(1) (1977), 11–14.

[8] Atta, A.G., Abd-Elhameed, W.M., Moatimid, G.M. and Youssri, Y.H. *Shifted fifth-kind Chebyshev Galerkin treatment for linear hyperbolic first-order partial differential equations*, Appl. Numer. Math., 167 (2021), 237–256.

[9] Atta, A.G. and Youssri, Y.H. *Advanced shifted first-kind Chebyshev collocation approach for solving the nonlinear time-fractional partial integro-differential equation with a weakly singular kernel*, Comput. Appl. Math., 41(8) (2022), 381.

[10] Aziz, T., Khan, A. and Rashidinia, J. *Spline methods for the solution of fourth-order parabolic partial differential equations*, Appl. Math. Comput., 167(1) (2005), 153–166.

[11] Bassuony, M.A., Doha, E.H., Abd-Elhameed, W.M. and Youssri, Y.H. *A Legendre-Laguerre-Galerkin method for the uniform Euler-Bernoulli beam equation*, East Asian J. Appl. Math., 8(2) (2018), 280–295.

[12] Evans, D.J. *A stable explicit method for the finite-difference solution of a fourth-order parabolic partial differential equation*, Comput. J., 8(3) (1965), 280–287.

[13] Evans, D.J. and Yousif, W.S. *A note on solving the fourth-order parabolic equation by the age method*, Int. J. Comput. Math., 40(1-2) (1991), 93–97.

[14] Fernandez, A., Restrepo, J.E. and Suragan, D. *A new representation for the solutions of fractional differential equations with variable coefficients*, Mediterr. J. Math., 20(1) (2023), 27.

[15] Han, S.M., Benaroya, H. and Wei, T. *Dynamics of transversely vibrating beams using four engineering theories*, J. Sound Vib., 225(5) (1999), 935–988.

[16] Heydari, M.H. and Hosseininia, M. *An efficient Jacobi spectral method for variable-order time fractional 2D Wu-Zhang system*, Comput. Math. Appl., 140 (2023), 89–106.

[17] Hilfer, R. *Applications of Fractional Calculus in Physics*, World Scientific, 2000.

[18] Hosseininia, M., Heydari, M.H., Baleanu, D. and Bayram, M. *A hybrid method based on the classical/piecewise Chebyshev cardinal functions for multi-dimensional fractional Rayleigh–Stokes equations*, Results Appl. Math., 25 (2025), 100541.

[19] Hosseininia, M., Heydari, M.H. and Razzaghi, M. *A hybrid spectral approach based on 2D cardinal and classical second-kind Chebyshev polynomials for time-fractional 3D Sobolev equation*, Math. Methods Appl. Sci., 46(18) (2023), 18768–18788.

[20] Jie, S. *Efficient spectral-Galerkin II. Direct solvers for second- and fourth-order equations by using Chebyshev polynomials*, SIAM J. Sci. Comput., 16 (1) (1995), 74–87.

[21] Mason, J.C. and Handscomb, D.C. *Chebyshev polynomials*, Chapman and Hall/CRC, 2002.

[22] Moustafa, M., Youssri, Y.H. and Atta, A.G. *Explicit Chebyshev-Galerkin scheme for the time-fractional diffusion equation*, Int. J. Mod. Phys. C, 35 (2024).

[23] Podlubny, I. *Fractional differential equations: An introduction to fractional derivatives, fractional differential equations, to methods of their solution and some of their applications*, Elsevier, 1998.

[24] Roul, P. and Goura, V.M.K.P. *A high-order numerical method and its convergence for time-fractional fourth-order partial differential equations*, Appl. Math. Comput., 366 (2020), 124727.

[25] Sajjadi, S.A., Najafi, H.S. and Aminikhah, H. *A numerical study on the non-smooth solutions of the nonlinear weakly singular fractional Volterra integro-differential equations*, Math. Methods Appl. Sci., 46(4) (2023), 4070–4084.

[26] Salama, M.H., Zedan, H.A., Abd-Elhameed, W.M., Youssri, Y.H. *Shifted Lucas polynomial-driven Tau approach for the telegraph equation: theoretical and numerical insights into accuracy and stability*, Comp. Appl. Math., 45 (2026), 397.

[27] Siddiqi, S.S. and Arshed, S. *Numerical solution of time-fractional fourth-order partial differential equations*, Int. J. Comput. Math., 92(7) (2015), 1496–1518.

[28] Sun, Z.Z. and Gao, G.H. *Fractional differential equations*, De Gruyter, 2020.

[29] Tariq, H. and Akram, G. *Quintic spline technique for time fractional fourth-order partial differential equation*, Numer. Methods Partial Differ. Equations, 33(2) (2017), 445–466.

[30] Wazwaz, A.M. *Analytic treatment for variable coefficient fourth-order parabolic partial differential equations*, Appl. Math. Comput., 123(2) (2001), 219–227.

[31] Xu, C., Farman, M. and Shehzad, A. *Analysis and chaotic behavior of a fish farming model with singular and non-singular kernel*, Int. J. Biomathematics, (2023), 2350105.

[32] Xu, C., Liao, M., Farman, M. and Shehzad, A. *Hydrogenolysis of glycerol by heterogeneous catalysis: a fractional order kinetic model with analysis*, MATCH Commun. Math. Comput. Chem., 91(3) (2024), 635–664.

[33] Xu, C., Lin, J., Zhao, Y., Cui, Q., Ou, W., Pang, Y., Liu, Z., Liao, M. and Li, P. *New results on bifurcation for fractional-order octonion-valued neural networks involving delays*, Network: Comput. Neur. Syst., 36 (2024), 545-597.

[34] Xu, C., Zhao, Y., Lin, J., Pang, Y., Liu, Z., Shen, J., Liao, M., Li, P. and Qin, Y. *Bifurcation investigation and control scheme of fractional neural networks owning multiple delays*, Comput. Appl. Math., 43(4) (2024), 1–33.

[35] Youssri, Y.H., Abd-Elhameed, W.M. and Atta, A.G. *Spectral Galerkin treatment of linear one-dimensional telegraph type problem via the generalized Lucas polynomials*, Arab J. Math., 11(3) (2022), 601–615.

[36] Youssri, Y.H., Abd-Elhameed, W.M., Elmasry, A.A. and Atta, A.G. *An efficient Petrov-Galerkin scheme for the Euler-Bernoulli beam equation via second-kind Chebyshev polynomials*, Fractal Fract., 9(2) (2025), 78.

[37] Youssri, Y.H. and Atta, A.G. *Spectral collocation approach via normalized shifted Jacobi polynomials for the nonlinear Lane-Emden equation with fractal-fractional derivative*, Fractal Fract., 7(2) (2023), 133.

[38] Youssri, Y.H. and Muttardi, M.M. *A mingled tau-finite difference method for stochastic first-order partial differential equations*, Int. J. Appl. Comput. Math., 9(2) (2023), 14.

[39] Zhao, X., Wang, L. and Xie, Z. *Sharp error bounds for Jacobi expansions and Gegenbauer–Gauss quadrature of analytic functions*, SIAM J. Numer. Anal., 51(3) (2013), 1443–1469.